arXiv:1602.05280v1 [cond-mat.stat-mech] 17 Feb 2016

Multifractality and Laplace spectrum of horizontal visibility graphs constructed from fractional Brownian motions

Zu-Guo Yu[1,2*], Huan Zhang[1], Da-Wen Huang[1], Yong Lin[3] and Vo Anh[2]

[1]Hunan Key Laboratory for Computation and Simulation in Science and Engineering and Key Laboratory of Intelligent Computing and Information Processing of Ministry of Education, Xiangtan University, Xiangtan, Hunan 411105, China.

[2]School of Mathematical Sciences, Queensland University of Technology, GPO Box 2434, Brisbane, Q4001, Australia.

[3]Department of Mathematics, School of Information, Remin University of China, Beijing 100872, China.

Abstract

Many studies have shown that additional information can be gained on time series by investigating their associated complex networks. In this work, we investigate the multifractal property and Laplace spectrum of the horizontal visibility graphs (HVGs) constructed from fractional Brownian motions. We aim to identify via simulation and curve fitting the form of these properties in terms of the Hurst index H. First, we use the sandbox algorithm to study the multifractality of these HVGs. It is found that multifractality exists in these HVGs. We find that the average fractal dimension $\langle D(0)\rangle$ of HVGs approximately satisfies the prominent linear formula $\langle D(0)\rangle = 2 - H$; while the average information dimension $\langle D(1)\rangle$ and average correlation dimension $\langle D(2)\rangle$ are all approximately bi-linear functions of H when $H \geq 0.15$. Then, we calculate the spectrum and energy for the general Laplacian operator and normalized Laplacian operator of these HVGs. We find that, for the general Laplacian operator, the average logarithm of second-smallest eigenvalue $\langle \ln(u_2)\rangle$, the average logarithm of third-smallest eigenvalue $\langle \ln(u_3)\rangle$, and the average logarithm of maximum eigenvalue $\langle \ln(u_n)\rangle$ of these HVGs are approximately linear functions of H; while the average Laplacian energy $\langle E_{nL}\rangle$ is approximately a quadratic polynomial function of H. For the normalized Laplacian operator, $\langle \ln(u_2)\rangle$ and $\langle \ln(u_3)\rangle$ of these HVGs approximately satisfy linear functions of H; while $\langle \ln(u_n)\rangle$ and $\langle E_{nL}\rangle$ are approximately a 4th and cubic polynomial function of H respectively.

Key words: horizontal visibility graph, fractional Brownian motion, multifractal property, Laplacian spectrum, Laplacian energy.

PACS: 89.75.Hc, 05.45.Df, 47.53.+n

*Corresponding author, email: yuzg1970@yahoo.com

1 Introduction

Complex network theory has become one of the most important developments in statistical physics [1]. Many studies have shown that complex networks play an important role in characterizing complicated dynamic systems in nature and society [2]. Studies have shown that complex network theory may be an effective method to extract the information embedded in time series [3–8]. The advancement of network theory provides us with a new perspective to perform time series analysis [7,8]. Especially we can further understand the structural features and dynamics of complex systems by studying the basic topological properties of their networks. Researchers have proposed some algorithms to construct different complex networks from time series [9], such as complex networks from pseudoperiodic time series [3], visibility graphs (VG) [5] and horizontal visibility graphs (HVG) [6], state space networks [10], recurrence networks [7, 8, 11], nearest-neighbor networks [4, 12] and complex networks based on phase space reconstruction [13] .

Among the aforementioned methods, the visibility algorithm proposed by Lacasa *et al.* [5] has attracted many applications from diverse fields [14], including stock market indices [15, 16], human stride intervals [17], occurrence of hurricanes in the United States [18], foreign exchange rates [19], energy dissipation rates in three-dimensional fully developed turbulence [20], human heartbeat dynamics [21, 22], diagnostic EEG markers of Alzheimer's disease [23], and daily streamflow series [24]. A VG is obtained from the mapping of a time series into a network according to the visibility criterion [5, 17]: Two arbitrary data points (t_a, y_a) and (t_b, y_b) in the time series have visibility, and consequently become two connected vertices (or nodes) in the associated graph, if any other data point (t_c, y_c) such that $t_a < t_c < t_b$ fulfills

$$y_c < y_a + (y_b - y_a)\frac{t_c - t_a}{t_b - t_a}.$$

Time series is defined in the time domain and the discrete Fourier transform (DFT) is defined on the frequency domain, the VG is defined on the "visibility domain". The DFT decomposes a signal in a sum of vibration modes, the visibility algorithm decomposes a signal in a concatenation of graphs motifs, and the degree distribution simply makes a histogram of such "geometric modes". The visibility algorithm is a geometric (rather than integral) transform.

A preliminary analysis [5] has shown that the constructed VG inherits several properties of the series in its structure. Thereby, periodic time series convert into regular graphs, and random series into random graphs. Moreover, fractal time series convert into scale-free networks, enhancing the fact that a power-law degree distribution of its graph is related to the fractality of the time series. Then Luque *et al.* [6] proposed the HVG which is geometrically simpler and forms an analytically solvable version of VG. The HVG has been used to study the daily solar X-ray brightness data [25] and protein molecular dynamics [26] by our group.

Self-similar processes have been used to model fractal phenomena in different fields, ranging from physics, biology, economics to engineering [17]. Fractional Brownian motion (fBm) is a stochastic processes defined by $dX_t = \mu(t, X_t)dt + \sigma(t, X_t)dB_t^H$, where μ is the drift coefficient, σ is the diffusion coefficient. B_t^H is a Gaussian process, the index H is called Hurst exponent with $0 < H < 1$ after the British hydrologist H. E. Hurst. Note that for $H = 1/2$ we get the standard Brownian

motion (standard Wiener motion), which we shall further denote by W_t [27]. Variance of fBm is $\sigma^2 t^{2H}$. Variance also corresponds to mean squared displacement [28, 29], EX_t^2. If $H = 1/2$, the diffusion process is called normal diffusion and the variance of fBm is $\sigma^2 t$. This is the same as cases of Brownian motion and Brownian motion with constant drift, which means the mean squared displacement (MSD) of a particle is a linear function of time. If $1/2 < H < 1$, the diffusion process is called super-diffusion (Levy flight and geometric Brownian motion both belong to super-diffusion). If $0 < H < 1/2$, the diffusion process is called sub-diffusion. We can choose different diffusion process to model the data with various mean squared displacement [27–29]. Lacasa *et al.* [17] showed that the VGs derived from generic fBm series are scale-free, and proved that there exists a linear relation between the Hurst exponent H of the fBm and the exponent γ of the power law degree distribution in the associated VG. The visibility algorithm thus provides another method to compute the Hurst exponent and characterize fBm. Xie and Zhou [14] studied the relationship between the Hurst exponent of fBm and the topological properties (clustering coefficient and fractal dimension) of its converted HVG. Our group [30] studied the topological and fractal properties of the recurrence networks constructed from fBms.

Based on the self-similarity of fractal geometry [27, 31, 32], Song *et al.* [2] generalized the box-counting method and used it in the field of complex networks. As a generalization of fractal analysis, the tool of multifractal analysis (MFA) has a better performance on characterizing the complexity of complex networks in real applications. MFA has been widely applied in a variety of fields such as financial modeling [33, 34], biological systems [35–38], and geophysical data analysis [39–42]. In recent years, MFA also has been successfully used in complex networks and seems more powerful than fractal analysis. As a consequence of this trend, some algorithms have been proposed to calculate the mass exponent $\tau(q)$ and then study the multifractal properties of complex networks. Furuya and Yakubo [43] proposed an improved compact-box-burning algorithm for MFA of complex networks based on the algorithm introduced by Song *et al.* [44], and applied it to show that some networks have a multifractal structure. Almost at the same time, Wang *et al.* [45] proposed a modified fixed-size box-counting method to detect the multifractal behavior of some theoretical and real networks, including scale-free networks, small-world networks, random networks, and protein-protein interaction networks. Li *et al.* [46] improved the algorithm of Ref. [45] further and used it to investigate the multifractal properties of a family of fractal networks introduced by Gallos *et al.* [47]. Then Liu *et al.* [30] studied the fractal and multifractal properties of the recurrence networks constructed from fBms. Recently, Liu *et al.* [48] employed the sandbox (SB) algorithm which was proposed by Tél et al. [49] for MFA of complex networks. By comparing the numerical results and the theoretical ones of some networks, it was shown that the SB algorithm is the most effective, feasible and accurate algorithm to study the multifractal behavior and calculate the mass exponent of complex networks.

In another direction, spectral graph theory has a long history. One of the main goals in graph theory is to deduce the principal properties and structure of a graph from its graph spectrum. The eigenvalues of Laplacian operator are closely related to almost all major invariants of a graph, linking one extremal property to another [50]. There is no question that eigenvalues play a central role in

our fundamental understanding of graphs [50]. The study of graph eigenvalues realizes increasingly rich connections with many other areas of mathematics. A particularly important development is the interaction between spectral graph theory and differential geometry [50, 51].

In this work, we investigate the multifractal property and Laplace spectrum of the HVGs constructed from fBms. First, we use the SB algorithm employed by Liu *et al.* [48] to study the multifractality of these HVGs. We then calculate the spectrum [50, 51] and energy [52] for the general Laplacian operator and normalized Laplacian operator of these HVGs. We aim to identify the functional forms of possible relationships between the Hurst index of the fBm and the multifractal indices, Laplacian spectrum and energy of the associated HVG.

2 Horizontal visibility graph of time series

A graph (or network) is a collection of vertices or nodes, which denote the elements of a system, and links or edges, which identify the relations or interactions among these elements. A large number of real networks are referred to as *scale-free* because the probability distribution $P(k)$ of the number of links per node (also known as the degree distribution) satisfies a power law $P(k) \sim k^{-\gamma}$ with the degree exponent γ varying in the range $2 < \gamma < 3$ [53].

Luque *et al.* [6] proposed the horizontal visibility graph (HVG) which are geometrically simpler and analytically a solvable version of VG [5]. Given a time series $\{x_1, x_2, ..., x_n\}$, two arbitrary data points x_i and x_j in the time series have horizontal visibility, and consequently become two connected vertices (or nodes) in the associated graph, if any other data point x_k such that $i < k < j$ fulfils

$$x_i, x_j > x_k.$$

Thus a connected, unweighted network could be constructed based on a time series and is called its horizontal visibility graph (HVG). Two nodes i and j in the HVG are connected if one can draw a horizontal line in the time series joining x_i and x_j that does not intersect any intermediate data height. Given a time series, its HVG is always a subgraph of its associated VG. Luque *et al.* [6] showed that the degree distribution of an HVG constructed from any random series has an exponential form $P(k) = (3/4)exp(-k\ln(3/2))$. Then Lacasa *et al.* [54] used the horizontal visibility algorithm to characterize and distinguish between correlated, uncorrelated and chaotic processes. They showed that horizontal visibility algorithm is able to distinguish chaotic series from independent and identically distributed (i.i.d.) theory without needs for additional techniques such as surrogate data or noise reduction methods [54]. Xie and Zhou [14] studied the relationship between the Hurst index of fBm and the topological properties (clustering coefficient and fractal dimension) of its converted HVG. In this work, we investigate the multifractal property, Laplace spectrum and energy of HVGs constructed from fBms.

3 Sandbox algorithm for multifractal analysis of complex networks

The fixed-size box-covering algorithm [55] is well known as one of the most common and important algorithms for MFA. For a given measures μ with support set E_0 in a metric space, we consider the

following partition sum

$$Z_\epsilon(q) = \sum_{\mu(B)\neq 0} [\mu(B)]^q, \tag{1}$$

$q \in R$, where the sum runs over all different nonempty boxes B of a given size ϵ in a box covering of the support set E_0. The mass exponents $\tau(q)$ of the measure μ can be defined as

$$\tau(q) = \lim_{\epsilon\to 0} \frac{\ln Z_\epsilon(q)}{\ln \epsilon}. \tag{2}$$

Then the generalized fractal dimensions $D(q)$ of the measure μ are defined as

$$D(q) = \frac{\tau(q)}{q-1}, \qquad \text{for} \quad q \neq 1, \tag{3}$$

and

$$D(q) = \lim_{\epsilon\to 0} \frac{Z_{1,\epsilon}}{\ln \epsilon}, \quad \text{for} \quad q = 1, \tag{4}$$

where $Z_{1,\epsilon} = \sum_{\mu(B)\neq 0} \mu(B) \ln \mu(B)$. Linear regression of $[\ln Z_\epsilon(q)]/(q-1)$ against $\ln \epsilon$ for $q \neq 1$ gives estimates of the generalized fractal dimensions $D(q)$, and similarly a linear regression of $Z_{1,\epsilon}$ against $\ln \epsilon$ for $q = 1$. In particular, $D(0)$ is the box-counting dimension (or fractal dimension), $D(1)$ is the information dimension, and $D(2)$ is the correlation dimension. Usually the strength of the multifractality can be measured by $\Delta D(q) = \max D(q) - \min D(q)$.

In a complex network, the measure μ of each box can be defined as the ratio of the number of nodes covered by the box and the total number of nodes in the entire network. In addition, we can determine the multifractality of complex network by the shape of the $\tau(q)$ or $D(q)$ curve. If $D(q)$ is a constant or $\tau(q)$ is a straight line, the object is monofractal; on the other hand, if $D(q)$ or $\tau(q)$ is convex, the object is multifractal.

The sandbox (SB) algorithm proposed by Tél *et al.* [49] is an extension of the box-counting algorithm [55]. The main idea of this sandbox algorithm is that we can randomly select a point on the fractal object as the center of a sandbox and then count the number of points in the sandbox. The generalized fractal dimensions $D(q)$ are defined as

$$D_q = \lim_{r\to 0} \frac{\ln\langle [M(r)/M(0)]^{q-1}\rangle}{\ln(r/d)} \frac{1}{q-1}, \qquad q \in R, \tag{5}$$

where $M(r)$ is the number of points in a sandbox with a radius of r, $M(0)$ is the total number of points in the fractal object. The brackets $\langle\cdot\rangle$ mean to take statistical average over randomly chosen centers of the sandboxes. In fact, the above equation can be rewritten as

$$\ln(\langle [M(r)]^{q-1}\rangle) \;\propto\; D(q)(q-1)\ln(r/d) + (q-1)\ln(M_0). \tag{6}$$

So, in practice, we often estimate numerically the generalized fractal dimensions $D(q)$ by performing a linear regression of $\ln(\langle [M(r)]^{q-1}\rangle)$ against $(q-1)\ln(r/d)$; and estimate numerically the mass exponents $\tau(q)$ by performing a linear regression of $\ln(\langle [M(r)]^{q-1}\rangle)$ against $\ln(r/d)$.

Recently, Liu *et al.* [48] proposed to employ the sandbox algorithm for MFA of complex networks. Before we use the following SB algorithm to perform MFA of a network, we need to apply Floyd's algorithm [56] of Matlab-BGL toolbox [57] to calculate the shortest-path distance matrix of this network according to its adjacency matrix A. The SB algorithm for MFA of complex networks [48] can be described as follows.

(i) Initially, make sure all nodes in the entire network are not selected as a center of a sandbox.

(ii) Set the radius r of the sandbox which will be used to cover the nodes in the range $r \in [1, d]$, where d is the diameter of the network.

(iii) Rearrange the nodes of the entire network into random order. More specifically, in a random order, nodes which will be selected as the center of a sandbox are randomly arrayed.

(iv) According to the size n of networks, choose the first 1000 nodes in a random order as the center of 1000 sandboxes, then search all the neighbor nodes by radius r from the center of each sandbox.

(v) Count the number of nodes in each sandbox of radius r, denote the number of nodes in each sandbox as $M(r)$.

(vi) Calculate the statistical average $\langle [M(r)]^{q-1} \rangle$ of $[M(r)]^{q-1}$ over all 1000 sandboxes of radius r.

(vii) For different values of r, repeat steps (ii) to (vi) to calculate the statistical average $\langle [M(r)]^{q-1} \rangle$ and then use $\langle [M(r)]^{q-1} \rangle$ for linear regression.

We need to choose an appropriate range of $r \in [r_{min}, r_{max}]$, then calculate the generalized fractal dimensions $D(q)$ and the mass exponents $\tau(q)$ in this scaling range. In our calculation, we perform a linear regression of $\ln(\langle [M(r)]^{q-1} \rangle)$ against $\ln(r)$ and then choose the slope as an approximation of the mass exponent $\tau(q)$ (the process for estimating the generalized fractal dimensions $D(q)$ is similar).

By comparing the numerical results and the theoretical ones of some networks, Liu *et al.* [48] showed that the SB algorithm is the most effective, feasible and accurate algorithm to study the multifractal behavior and calculate the mass exponents of complex networks. Hence we use the SB algorithm employed by Liu *et al.* [48] to study the multifractality of the HVGs constructed from fBms in this work.

4 Laplacian spectrum and energy of complex networks

Suppose G is a undirected graph with vertex set V and edge set E. The distance between two vertices is the minimum number of edges to connect them; the diameter of G is the maximum of all the distances of the graph [51].

Denote the adjacent matrix of the graph G as $A = (a_{ij})_{n \times n}$, the degree of vertex i as d_i. T is diagonal matrix of degrees, i.e.

$$T = \begin{pmatrix} d_1 & 0 & \cdots & 0 \\ 0 & d_2 & \cdots & 0 \\ \vdots & \vdots & \ddots & \vdots \\ 0 & 0 & \cdots & d_n \end{pmatrix} \tag{7}$$

Define the operator $L = (b_{ij})_{n\times n}$, where

$$b_{ij} = \begin{cases} d_i, & if\ i = j \\ -1, & if\ a_{ij} = 1 \\ 0, & others \end{cases} \tag{8}$$

It is obvious that $L = T - A$. This operator L is the general Laplace operator. The normalized Laplace operator $\mathcal{L}$ is defined as $\mathcal{L} = (c_{ij})_{n\times n}$ [50], where

$$c_{ij} = \begin{cases} 1, & if\ i = j \\ -\frac{1}{\sqrt{d_i d_j}}, & if\ a_{ij} = 1 \\ 0, & others \end{cases} \tag{9}$$

Denote

$$T^{-\frac{1}{2}} = \begin{pmatrix} d_1^{-\frac{1}{2}} & 0 & \cdots & 0 \\ 0 & d_2^{-\frac{1}{2}} & \cdots & 0 \\ \vdots & \vdots & \ddots & \vdots \\ 0 & 0 & \cdots & d_n^{-\frac{1}{2}} \end{pmatrix} \tag{10}$$

where we set $d_i^{-1} = 0$ when $d_i = 0$. It is seen that $\mathcal{L} = T^{-\frac{1}{2}} L T^{-\frac{1}{2}}$. The spectrum consists of the eigenvalues of the general Laplacian operator L and normalized Laplacian operator $\mathcal{L}$ of the graph. It can be proved that the smallest eigenvalue u_1 of the general Laplacian operator L and normalized Laplacian operator $\mathcal{L}$ of a connected graph is equal to 0 [50, 51]. Usually, the second smallest eigenvalue u_2 and the maximum eigenvalue u_n have particular meaning. The second smallest eigenvalue $u_2 = u_2 - u_1$ (because $u_1 = 0$) is called the Laplacian spectral gap [51]. The second smallest eigenvalue u_2 and maximum eigenvalue u_n are related to the synchronizability of complex networks [58]. Hence we pay more attention to the second-smallest eigenvalue u_2, the third-smallest eigenvalue u_3, the average maximum eigenvalue u_n of these two Laplacian operators of a graph in this work.

The Laplacian energy [52] , E_{nL}, is defined as

$$E_{nL} = \Sigma_{i=1}^{n} |u_i - \frac{2m}{n}|. \tag{11}$$

where u_i is the ith eigenvalue of the general Laplacian operator L (or normalized Laplacian operator $\mathcal{L}$) of the graph, n and m are the numbers of vertices and edges in the graph respectively.

5 Results and discussion

In this work, we use the Matlab command "wfbm" to generate fBm time series of parameter H ($0 < H < 1$) and length n following the wavelet-based algorithm proposed by Abry and Sellan [59]. We consider fBm time series with length $n = 10^4$ and different Hurst indices H ranging from 0.05 to 0.95 (the step difference is 0.05). For each value of Hurst index H, we generate 100 fBm time series with the same H, then we convert them into 100 HVGs.

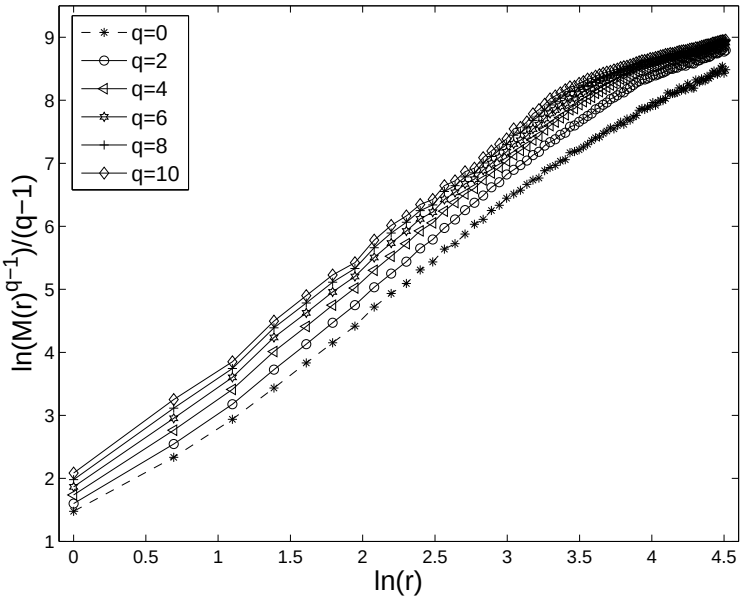

Figure 1: Linear regressions for calculating the generalized dimensions $D(q)$ of a HVG converted from a fBm time series with Hurst index $H = 0.4$.

For each HVG, we calculate the $D(q)$ and $\tau(q)$ curves using the SB algorithm. We calculate the $D(q)$ and $\tau(q)$ curves with q ranging from -10 to 10 (the step difference is set to 1/3). After checking carefully many times with visual inspection, we find the best linear regression range of r is $r \in (20, 72)$ in our setting. Hence we set the range $r \in (20, 72)$ in our computations. We provide the linear regression to estimate $D(q)$ for a HVG converted from a fBm time series with Hurst index $H = 0.4$ in Figure 1 as an example.

In the following, the averages are taken over HVGs constructed from 100 time series of fBm with the same Hurst index H. We show the average $\langle \tau(q) \rangle$ curves and average $\langle D(q) \rangle$ curves in Figure 2. From Figure 2, we find that the $\langle \tau(q) \rangle$ and $\langle D(q) \rangle$ curves of HVGs are not straight lines, hence asserting that multifractality exists in these HVGs constructed from fBm series. We also find that the average multifractality of these HVGs becomes weaker, which is indicated by the value of $\langle \Delta D(q) \rangle = \langle D(-10) - D(10) \rangle$, when the Hurst index of the given time series increases, and the average multifractality is approximately a quadratic polynomial function of H when $H \geq 0.1$ (as shown in the left panel of Figure 3).

The estimated average values of $D(0)$, $D(1)$ and $D(2)$ of HVGs constructed from fBm time series with different Hurst indices H are given in Table 1.

We show the relationship between the Hurst index H and the average fractal dimension $\langle D(0) \rangle$ in the right panel of Figure 3. We can see that the average fractal dimension $\langle D(0) \rangle$ decreases with increasing H. Furthermore, it is pleasing that the curve shows a nice linear relationship:

$$\langle D(0) \rangle = 2.007 - 1.0184 * H,$$

when $H \geq 0.15$, which approximates the theoretical relationship between the Hurst index H and the fractal dimension d of the graph of fBm $d = 2 - H$. Our numerical results show that the fractal dimension of the constructed HVGs approximates closely that of the graph of the original fBm. In

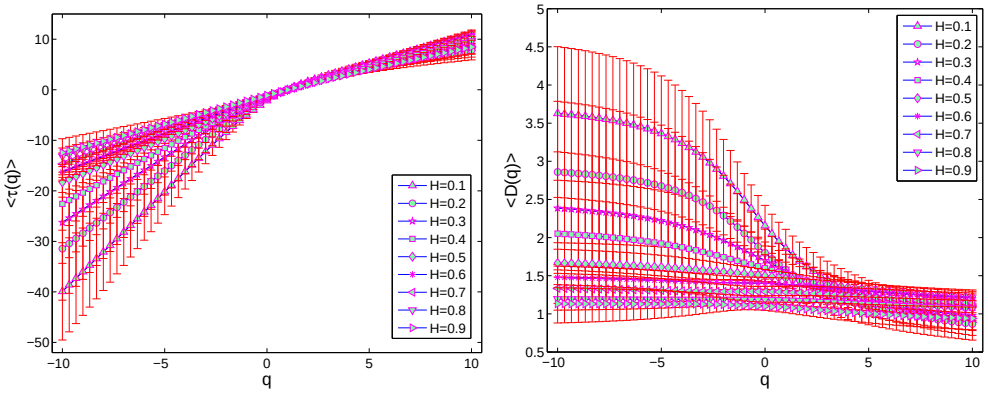

Figure 2: The average $\langle \tau(q) \rangle$ **(Left)** and $\langle D(q) \rangle$ **(Right)** curves of the HVGs. Here the average is calculated from 100 realizations, and error bars are calculated by the standard errors.

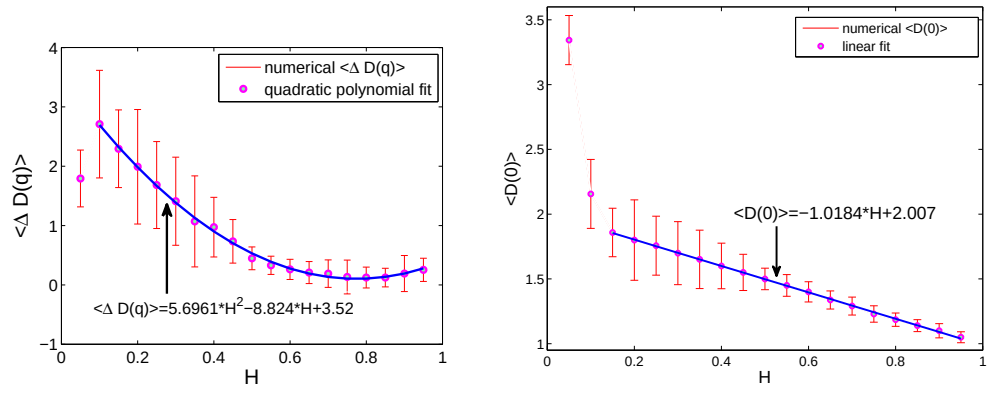

Figure 3: The relationship between H of fBm and average multifractality $\langle \Delta D(q) \rangle$ **(Left)**, and average fractal dimension $\langle D(0) \rangle$ **(Right)** of the associated HVGs. Here the average is calculated from 100 realizations, and error bars are calculated by the standard errors.

Table 1: The average value of $D(0)$, $D(1)$, $D(2)$ and $\Delta D(q)$ of HVGs constructed from fBm time series with different Hurst index H. Here the average is calculated from 100 realizations.

H	$\langle D(0)\rangle$	$\langle D(1)\rangle$	$\langle D(2)\rangle$	$\langle \Delta D(q)\rangle$
0.20	1.7997959	1.5762884	1.3987674	1.9911429
0.25	1.7566540	1.5838531	1.4341853	1.6833939
0.30	1.6987564	1.5615922	1.4340036	1.4104275
0.35	1.6510399	1.5385958	1.4319206	1.0708452
0.40	1.6000885	1.5199201	1.4358003	0.9740916
0.45	1.5502299	1.4933475	1.4299984	0.7340563
0.50	1.4997731	1.4635467	1.4240391	0.4474166
0.55	1.4496548	1.4282816	1.4010555	0.3302060
0.60	1.4000067	1.3872357	1.3679190	0.2620100
0.65	1.3376393	1.3306918	1.3179500	0.2078157
0.70	1.2907005	1.2839972	1.2721686	0.1899058
0.75	1.2291436	1.2247421	1.2173406	0.1339882
0.80	1.1857852	1.1793346	1.1696728	0.1273265
0.85	1.1394171	1.1295888	1.1174955	0.1238226
0.90	1.1000428	1.0834080	1.0638481	0.1914100
0.95	1.0499715	1.0178998	0.9860908	0.2535463

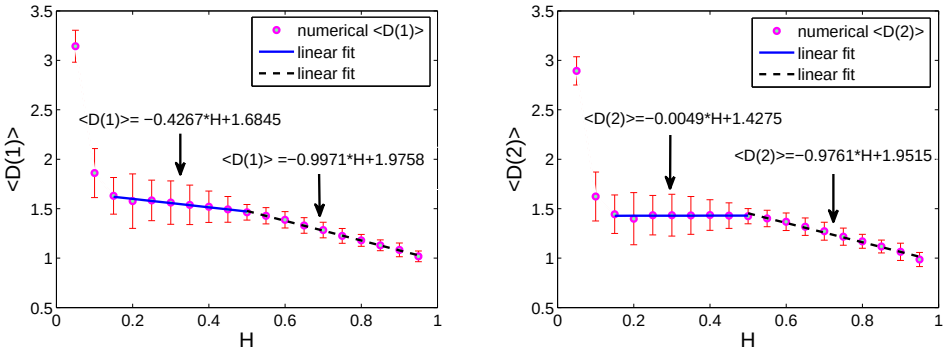

Figure 4: The relationship between H of fBm and average information dimension $\langle D(1)\rangle$ (**Left**), and average correlation dimension $\langle D(2)\langle$ (**Right**) of the associated HVGs. Here the average is calculated from 100 realizations, and error bars are calculated by the standard errors.

other words, the fractality of the fBm is inherited in their HVGs. This result was also reported by Xie and Zhou [14], where they calculated the fractal dimension of HVGs by the simulated annealing algorithm. The functional relationships of the average information dimension $\langle D(1)\rangle$ and the average correlation dimension $\langle D(2)\rangle$ with the Hurst index H are given in Figure 4. As shown in Figure 4, we find that these relationships can be well fitted by the following bi-linear functions:

$$\langle D(1)\rangle = \begin{cases} -0.4267 * H + 1.6845, & when\ 0.15 \leq H \leq 0.5, \\ -0.9971 * H + 1.9758, & when\ 0.5 \leq H \leq 0.95 \end{cases}$$

and

$$\langle D(2)\rangle = \begin{cases} -0.0049 * H + 1.4275, & when\ 0.15 \leq H \leq 0.5, \\ -0.9761 * H + 1.9515, & when\ 0.5 \leq H \leq 0.95. \end{cases}$$

Then we calculate the spectrum [50, 51] and energy [52] for the general Laplacian operator and normalized Laplacian operator of these HVGs. One can see that all the HVGs constructed are connected. The smallest eigenvalue u_1 of the general Laplacian operator L and normalized Laplacian operator $\mathcal{L}$ of a connected graph is equal to 0. Because the second smallest eigenvalue u_2 and the maximum eigenvalue u_n have particular meaning, we pay more attention to the second-smallest eigenvalue u_2, the third-smallest eigenvalue u_3, the average maximum eigenvalue u_n of these two Laplacian operators of a graph in this work. We find that for the general Laplacian operator, the average logarithm of second-smallest eigenvalue $\langle \ln(u_2)\rangle$, the average logarithm of third-smallest eigenvalue $\langle \ln(u_3)\rangle$, and the average logarithm of maximum eigenvalue $\langle \ln(u_n)\rangle$ of these HVGs are approximately linear functions of H; while the average Laplacian energy $\langle E_{nL}\rangle$ is approximately a quadratic polynomial function of H. We show these relationships in Figure 5. For the normalized Laplacian operator, $\langle \ln(u_2)\rangle$ and $\langle \ln(u_3)\rangle$ of these HVGs approximately satisfy linear functions of H; while $\langle \ln(u_n)\rangle$ and $\langle E_{nL}\rangle$ are approximately a 4th and cubic polynomial function of H respectively. These relationships are shown in Figure 6.

From the above results, we conclude that the inherent nature of the time series affects the structure characteristics of the associated networks and the dependence relationships between them appear retained. Our work supports that complex networks provide a suitable and effective tool to

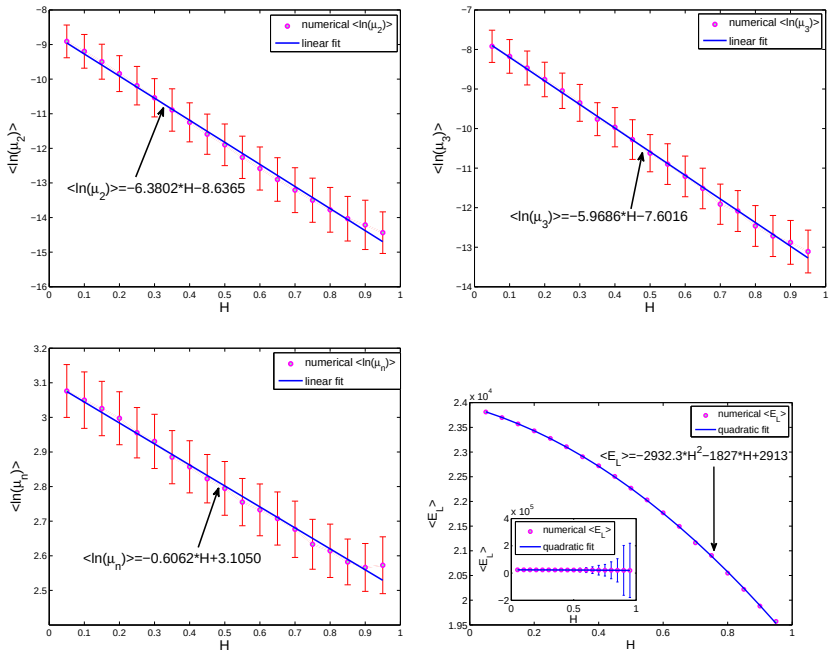

Figure 5: The relationship between H of fBm and average logarithm of second-smallest eigenvalue $\langle \ln(u_2) \rangle$, average logarithm of third-smallest eigenvalue $\langle \ln(u_3) \rangle$, average logarithm of maximum eigenvalue $\langle \ln(u_n) \rangle$, and average Laplacian energy $\langle E_{nL} \rangle$ of these HVGs for general Laplacian operator. Here the average is calculated from 100 realizations, and error bars are calculated by the standard errors.

perform time series analysis.

Acknowledgments

This project was supported by the Natural Science Foundation of China (Grant no. 11371016), the Chinese Program for Changjiang Scholars and Innovative Research Team in University (PCSIRT) (Grant No. IRT1179).

References

[1] Albert R and Barabási A L, 2002 *Rev. Mod. Phys.* **74** 47
[2] Song C, Havlin S, and Makse H A, 2005 *Nature* **433** 392
[3] Zhang J, Small M, 2006 *Phys. Rev. Lett.* **96** 238701
[4] Xu X -K, Zhang J, Small M, 2008 *Proc. Natl. Acad. Sci. USA* **105** 19601
[5] Lacasa L, Luque B, Ballesteros F, Luque J, Nuno J C, 2008 *Proc. Natl. Acad. Sci. USA* **105** 4972
[6] Luque B, Lacasa L, Ballesteros F, and Luque J, 2009 *Phys. Rev. E* **80** 046103
[7] Donner R V, Zou Y, Donges J F, Marwan N, and Kurths J, 2010 *New J. Phys.* **12** 033025
[8] Donner R V, Zou Y, Donges J F, Marwan N, and Kurths J, 2010 *Phys. Rev. E* **81** 015101(R)
[9] Small M, Zhang J, and Xu X K, 2009 *in: Lect. Notes Institue Comput. Sci. Soc. Infor. Telecommun. Engineering* **5** 2078
[10] Li C B, Yang H, and Komatsuzaki T, 2008 *Proc. Natl. Acad. Sci. USA.* **105** 536
[11] Marwan N, Donges J F, Zou Y, Donner R V, and Kurths J, 2009 *Phys. Lett. A* **373** 4246
[12] Liu C and Zhou W X, 2010 *J. Phys. A* **43** 495005
[13] Gao Z -K, Jin N -D, 2009 *Chaos* **19** 033137

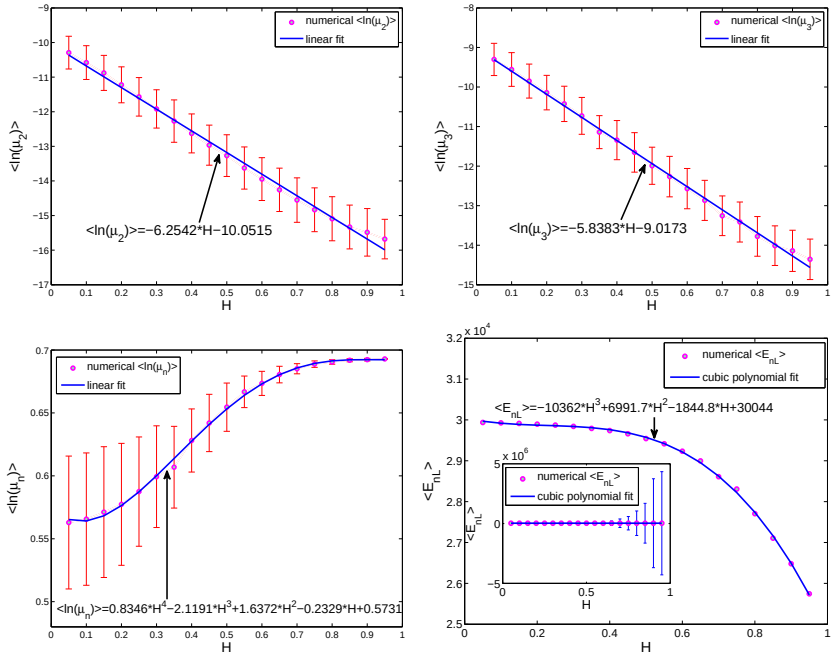

Figure 6: The relationship between H of fBm and average logarithm of second-smallest eigenvalue $\langle \ln(u_2) \rangle$, average logarithm of third-smallest eigenvalue $\langle \ln(u_3) \rangle$, average logarithm of maximum eigenvalue $\langle \ln(u_n) \rangle$, and average Laplacian energy $\langle E_{nL} \rangle$ of these HVGs for normalized Laplacian operator. Here the average is calculated from 100 realizations, and error bars are calculated by the standard errors.

[14] Xie W J and Zhou W X, 2011 *Physica A* **390** 3592
[15] Ni X -H, Jiang Z -Q, Zhou W -X, 2009 *Phys. Lett. A* **373** 3822
[16] Qian M -C, Jiang Z -Q, Zhou W -X, 2010 *J. Phys. A* **43** 335002
[17] Lacasa L, Luque B, Luque J, and Nuño J C, 2009 *Europhys. Lett.* **86** 30001
[18] Elsner J B, Jagger T H, Fogarty E A, 2009 *Geophys. Res. Lett.* **36** L16702
[19] Yang Y, Wang J -B, Yang H -J, Mang J -S, 2009 *Physica A* **388** 4431
[20] Liu C, Zhou W -X, Yuan W -K, 2010 *Physica A* **389** 2675
[21] Shao Z -G, 2010 *Appl. Phys. Lett.* **96** 073703.
[22] Dong Z, Li X, 2010 *Appl. Phys. Lett.* **96** 266101.
[23] Ahmadlou M, Adeli H, Adeli A, 2010 *J. Neural Transform.* **117** 1099
[24] Tang Q, Liu J, Liu H -L, 2010 *Modern Phys. Lett. B* **24** 1541
[25] Yu Z G, Anh V Eastes R and Wang D L, 2012 *Nonlin. Process. Geophys.* **19** 657
[26] Zhou Y W, Liu J L, Yu Z G, Zhao Z Q and Anh V, 2014 *Physica A* **416** 21
[27] Mandelbrot B B, 1983 *The Fractal Geometry of Nature* (New York: Academic Press)
[28] Makse H A, Davies G W, Havlin S, Ivanov P C, King P R, and Stanley H E, 1996 *Phys. Rev. E* **54** 3129
[29] Rybski D, Buldyrev S V, Havlin S, Liljeros F and Makse H A 2012 *Scientific Reports* **2** 560
[30] Liu J L, Yu Z G, and Anh V, 2014 *Phys. Rev. E* **89** 032814
[31] Feder J, 1988 *Fractals* (New York: Plenum)
[32] Falconer K, 1997 *Techniques in Fractal Geometry* (New York: Wiley)
[33] Canessa E, 2000 *J. Phys. A: Math. Gen.* **33** 3637
[34] Anh V V, Tieng Q M, and Tse Y K, 2000 *Int. Trans. Oper. Res.* **7** 349
[35] Yu Z G, Anh V and Lau K S, 2001 *Phys. Rev. E* **64** 031903
[36] Yu Z G, Anh V and Lau K S, 2003 *Phys. Rev. E* **68** 021913
[37] Yu Z G, Anh V and Lau K S, 2004 *J. Theor. Biol.* **226** 341
[38] Yu Z G, Anh V, Lau K S and Zhou L Q, 2006 *Phys. Rev. E* **73** 031920
[39] Yu Z G, Anh V V, Wanliss J A and Watson S M, 2007 *Chaos, Solitons and Fractals* **31** 736

[40] Yu Z G, Anh V and Eastes R, 2009 *J. Geophys. Res.* **114** A05214
[41] Yu Z G, Anh V, Wang Y, Mao D, and Wanliss J, 2010 *J. Geophys. Res.* **115** A10219
[42] Yu Z G, Anh V and Eastes R, 2014 *J. Geophys. Res.:Space Physics* **119** 7577
[43] Furuya S and Yakubo K, 2011 *Phys. Rev. E* **84** 036118
[44] Song C, Gallos L K, Havlin S and Makse H A, 2007 *J. Stat. Mech.: Theor. Exp.* P03006
[45] Wang D L, Yu Z G, and Anh V, 2012 *Chin. Phys. B* **21(8)** 080504
[46] Li B G, Yu Z G, and Zhou Y, 2014 *J. Stat. Mech.: Theor. Exp.* P02020
[47] Gallos L K, Song C, Havlin S and Makse H A, 2007 *Proc. Natl. Acad. Sci. USA.* **104(19)** 7746
[48] Liu J L, Yu Z G, and Anh V, 2015 *Chaos* **25** 023103
[49] Tél T, Fülöp Á and Vicsek T, 1989 *Physica A* **159** 155
[50] Chung F R K, 1997 *Spectral Graph Theory* (CBMS Regional Conference Series in Mathematics, Number 92, American Mathematical Society)
[51] Lin Y and Yau S T, 2010 *Math. Res. Lett.* **17(2)** 345
[52] Gutman I and Zhou B, 2006 *Linear Algebra Appl.* **414(1)** 29
[53] Albert R, Jeong H, and Barabasi A L, 1999 *Nature* **401** 130
[54] Lacasa L, Toral R, 2010 *Phys. Rev. E* **82** 036120
[55] Halsey T C, Jensen M H, Kadanoff L P, Procaccia I, and Shraiman B I, 1986 *Phys. Rev. A* **33** 1141
[56] Floyd R W, 1962 *Commun. ACM* **5(6)** 345
[57] Gleich D F, *A graph library for Matlab based on the boost graph library, http://dgleich.github.com/matlab-bgl.*
[58] Atay F M, Biyikoglu T, Jost J, 2006 *Physica D* **224** 35
[59] Abry P, Sellan F, 1996 *Appl. and Comp. Harmonic Anal.* **3(4)** 377